1 Introduction

1.1 Motivation

The class of composite materials features a broad variety of starting constituents as well as processing and design strategies. Depending on the desired application, unique new properties of the composite can be tailored by choosing proper constituent materials and fabrication techniques. [1] A subcategory of advanced composite materials consists of nanoparticles embedded in a polymer matrix which leads to nanoparticle–polymer composites and receive a radical scientific advancement as well as technical relevance in engineering and consumer industry. [2] To obtain a functional material with high hardness and mechanical strength, composite materials are formed from polymers and the implementation of ceramic–like magnetic or conducting substances. [3] Nanocomposite materials consisting of inorganic scaffolds and polymers have become increasingly interesting due to the high variety of possible applications as functional materials, which combine the advantages of polymeric properties with inorganic mixed oxide features and open new fields of material usage. [4, 5]

Nanocomposite materials consisting of inorganic scaffolds and polymers have become increasingly interesting due to their high variety of possible applications as functional materials. Nanocomposites are usually prepared by the integration of nanoparticles into monomers or polymers by dispersing the particles into the liquid phase. [6] This approach leads to highly agglomerated compounds with limited percolation. High filler content is restricted by the strongly increasing viscosity which makes processing impossible. Therefore, it is difficult to improve composites properties which depend on particle–particle contacts, like electrical or thermal conductivity. [7–9]

Heretofore, nanoparticle–polymer composites where prepared by dispersing post–functionalized inorganic nanoparticles into a monomer solution. [10] This approach leads to highly agglomerated compounds with limited percolation capabilities. [11] Thus, the rather broadly distributed pore sizes and composition ranges limit the adequate deployment of these composites for particular tasks.

This restriction can be circumvented by the new concept of inverse nanocomposites. For this, in the first step a porous particle scaffold is prepared which ensures a high degree of particle–particle contacts, as depicted in Figure 1.1. [12] In this first step, a nanoparticle scaffold is created from either flame spray pyrolysis and subsequent layer–to–layer–transfer or *via* a sol–gel–process with a polymeric binder. These layers reveal high structural

resilience against exposure to liquids. [13] The pores of the scaffold with diameters from molecular level up to some micrometers are then filled with a monomer which is subsequently polymerized. [14]

The afore–mentioned preparational outline towards inversely prepared NPC films shows potential usability in multilayer nanomaterials tailored for corrosion protection. [15] Technically significant interest in such layers arises from the need for multi–component but structurally resistant release–on–demand systems in the field of nanomedicine. [16] As the material choice of nanoparticles for the inverse NPCs is governed by rather low restraints, nanoparticles with photochemical activity or optoelectronic response behavior allow for applications in optical sensing or imaging techniques. [17, 18]

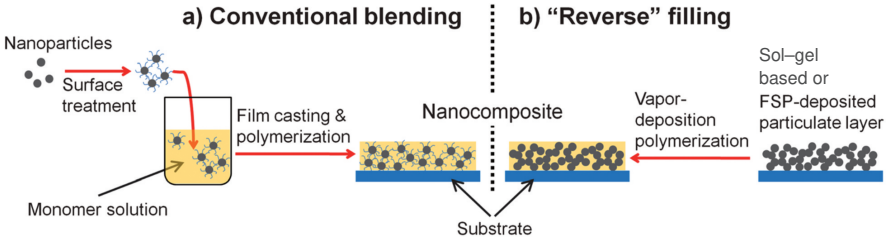

Figure 1.1. Routes for preparing NPC films based on inorganic nanoparticles and polymers. a) Dispersing surface–modified nanoparticles in polymer solution without particle–particle–contacts. (b) Pre–structuring of nanoparticle scaffold from FSP and vapor condensation leading to surface–initiated polymerization, believed to maintain initial particle connectivity. Reprinted with permission from Zhang *et al.* [12][2]

Nanoporous systems based on chemically inert particles like silica allow for controlling the pore size in a defined way leading to layers containing nanopores. [19] Under current aspects of ecological friendly and sustainable material research, inverse nanocomposites consisting of flexible polymers and electro optical nanoparticles lead the way towards biodegradable, printable, flexible and wearable electronics. [20–24] The field of possible applications for inverse nanocomposites grows with technical progress. [25, 26] These few presented examples for versatility of inverse nanocomposites emphasize the relevance of this study to gain insight into the structure–property relationships of this particular material class.

[2] Reprinted from Zhang, H., Popp, M., Hartwig, A., Mädler, L.: Synthesis of polymer/inorganic nanocomposite films using highly porous inorganic scaffolds. *Nanoscale* **4**(7), 2326–2332 (2012). doi: 10.1039/c2nr12029a, Copyright (2021), with permission from Royal Society of Chemistry provided by CCC under license number 1126418-1.

1.2 Scientific Question

The inverse nanoparticle–polymer composites possess great potential as a thin–film–material for photo catalysis, water–splitting reactions and biological sensors in liquid environments. To enable these applications, the knowledge about the structure–property relationship is crucial. [27] Before one can establish a continuous technological process of forming nanocomposite–films with tunable properties, a profound understanding of the molecular interactions is necessary. [28] However, this preparation process requires not only stable nanoparticle layers, but also fundamental knowledge of the occurring forces impacting the porous nanoparticle scaffold involved during liquid monomer imbibition. [29]

Recently, Mädler *et al.* [30] developed a new two–step layer transfer process for the fabrication of highly porous nanoparticle layers onto various substrates. The nanoparticles are synthesized in a Flame–Spray–Pyrolysis and transferred *via* low pressure lamination to various substrates leading to layers withstanding liquid environments. [31] These layers will be applied for monomer infiltration followed by polymerization. The occurring forces on the structure during imbibition are not studied in detail, yet. For this purpose, the imbibition properties of different liquids in nanoparticle layers will be analyzed in an experimental study and compared with a computational model of Baric. [32]

To form such systems based on gas phase synthesis, the inorganic particle framework will be prepared in a first step before it is exposed to the monomer followed by polymerization. Therefore, a highly porous percolating inorganic nanoparticle layer is synthesized *via* flame spray pyrolysis (FSP) and laminated onto a substrate foil or glass slide for immobilization. [30, 33] Examples for materials for FSP are Al_2O_3, $(In_2O_3)_{0.9}\cdot(SnO_2)_{0.1}$ (ITO), SiO_2, TiO_2 or WO_3 forming precursors. [31]

Furthermore, similar structures will be prepared on a wet chemical way. The nanoparticles will be dispersed in a solvent with some sol–gel–binder for subsequent imbibition with the monomer. [34] Both kinds of nanoporous layers will be used for imbibition with acrylic or epoxy based monomers followed by photopolymerization. [35] The polymerization shrinkage in nanoparticle layers and its influence on the particle–particle contacts will be studied. These studies enable the synthesis of nanoparticle–polymer composite materials with significantly lower particle contents but a higher number and increased quality of particle–particle–contacts compared to conventional composites having various applications as e.g. conductive, photocatalytic or adhesion promoting materials with polymer properties. [36]

To avoid these afore mentioned physical limitations, the new approach of the presented study is to form composite materials from highly porous nanoparticle layers withstanding

liquid environments instead of dispersing single particles in the monomer. This has the advantage of co–continuously distributed and already percolating nanoparticle structures in the matrix material. Thus, the effort of nanoparticle dispersion and the filling degree to reach the percolation threshold can be decreased. [37]

Through a four–step process, inverse nanocomposites could be prepared on two different routes. In the route of FSP–deposition, nanoparticle aggregates are created by FSP on a filter first. [38] Second, the nanoparticles are laminated onto a substrate by layer–to–layer transfer to form the nanoparticle layer. [31] Alternatively the nanoparticle layer can be created *via* a sol–gel–route. For this, the nanoparticles are dispersed and stabilized first together with a binder in solution. Subsequently the dispersion is doctor bladed on the target substrate in step number two. Both routes are complemented with monomer imbibition as third step and photopolymerization as final process step.

For the example of ITO particles, it could be shown that the electric conductivity increases if the pores are filled with the monomer (in other words by the addition of a non–conductive material) and a further strong increase is observed upon monomer polymerization. The conductivity increase is explained in the first step by increasing the number and quality of particle–particle contacts by capillary forces and in the second step by the polymerization shrinkage. In addition, influence of the "nanoscopic" compartments on the radical polymerization is shown as well as mechanical and thermomechanical properties of the obtained inverse nanocomposites.

Figure 1.2 denotes the two different processing methods towards mesoporous nanoparticle layers. Inverse nanocomposite is defined by us as a nanocomposite which is formed by first preparation of a particle scaffold which is afterwards infiltrated by the organic matrix material to be subsequently photopolymerized.

This path of the inverse nanocomposite synthesis is not fundamentally understood yet in a physicochemical way. That leads to the question how and why the structure and interaction of the inorganic scaffold alternates during the imbibition and polymerization processes. Furthermore, the influence of the scaffold on the polymerization and the formed polymer is an important question. [29]

The kinetics and physics will be evaluated by *in–situ* IR spectroscopy and the monomer turnover will be determined in dependence on the reaction time. Polymerization shrinkage and its structural influence will be examined by various microscopic methods.

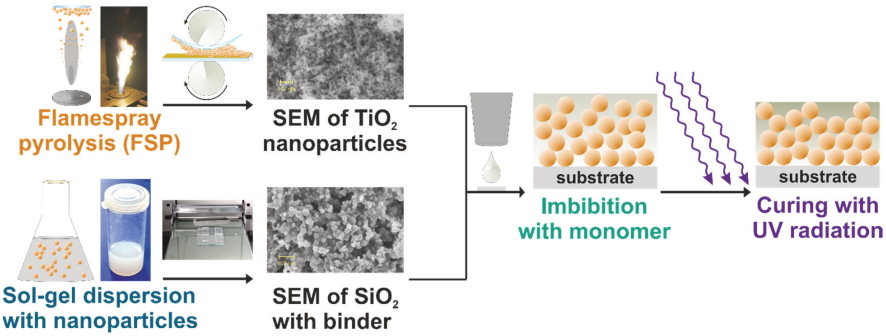

Figure 1.2. Preparation of inverse nanoparticle–polymer composites by formation of highly mesoporous nanoparticle scaffolds by either flame spray pyrolysis (FSP) or a wet–chemical sol–gel–process followed by monomer imbibition and subsequent polymerization *via* UV–irradiation. SEM images represent typical nanoparticle network structures prior to imbibition with monomer.

The density and pore size distribution changes may be controlled by varying the network structure of the polymer, which claims the variation of the linking moieties in the monomer. Further spectroscopic and rheological investigations will offer insight to shear and tensile strength, the ratio between capillary forces and surface tension. For electrically conducting materials like ITO, the conductance and impedance are measured before, during and after polymerization. The influences of in–process humidity on the surface interaction will be examined.

In the final part, the results of the different analytical investigations will be combined to gather an interpretation of the microscopic changes in forces and structure during the preparation of inverse nanocomposites. A comparison of both routes (FSP and sol–gel) for forming inverse NPC films concludes the presented investigation.

2 Theoretical Background

2.1 Porosity and Percolation

The formation of inverse NPC films is pre–defined by the structure of the nanoparticle scaffold. A major physical parameter which sets the material ratio and structure of the composite is described by the porosity Φ. This is defined as the fraction of pore space in the total volume. [39] Herein, the total pore volume $V_{P\mathrm{tot}}$ contains all classes of pores, closed, blind (dead–end), through and interconnected. The total volume V_{tot} includes all subsisting phases in the material. The non–porous material occupies the bulk volume V_{bulk}. According to Rouqerol *et al.*, [40] in this manuscript the porosity is defined as:

$$\Phi = \frac{V_{P\mathrm{tot}}}{V_{\mathrm{tot}}} = 1 - \frac{V_{\mathrm{bulk}}}{V_{\mathrm{tot}}} = 1 - \frac{\rho_{\mathrm{tot}}}{\rho_{\mathrm{bulk}}} \tag{2.1}$$

As the pore volume is difficult to measure, the porosity is calculated from the density ratio. Experimentally, the porosity is either calculated based on adsorption isotherm data or on macroscopic density measurements combined with microscopic data from transmission electron microscopy. The widely used approach of specific surface area determination bases on nitrogen adsorption by the isothermal Brunauer–Emmett–Teller method (BET). [41] When the spheric particle diameter d_s is known, and dense packing of perfect spheres represented by the coordination parameter $\xi = 6$, the specific surface area A_{BET} can be calculated from the density of the material ρ_{bulk}. However, the simple equation 2.2 is a rather rough estimation of the ratio between material density and porosity.

$$A_{\mathrm{BET}} = \frac{\xi}{\rho d_S} \tag{2.2}$$

With the Barrett–Joyner–Halenda method (BJH), [42] the total pore volume for cylindrical pores can be calculated from the adsorbed gas volume fraction υ_{adb}, when the nitrogen physisorption isotherms are evaluated with the *t*–curve method to obtain the adsorbed layer thickness t_j. [43]:

$$\upsilon_{\mathrm{adb}}\left({}^{p}/_{p_0}\right) = \sum_{j=1}^{k} \Delta V_j \left(r_j\left({}^{p}/_{p_0}\right)\right) + \sum_{j=k+1}^{n} A_{\mathrm{BET}} t_j \left(r_j\left({}^{p}/_{p_0}\right)\right) \tag{2.3}$$

From the BJH pore size distribution scheme, the total pore volume $V_{P\mathrm{tot}}$ follows as sum of all pore volume increments ΔV_j and thus, the porosity from gas adsorption can be calculated as follows:

$$\Phi = \frac{V_{P\mathrm{tot}}}{V_{P\mathrm{tot}} + \rho_{\mathrm{bulk}}^{-1}} \tag{2.4}$$

However, the model only covers the pore size range of mesopores with diameters between 3 – 500 nm. [13] Micropores (>0.5 µm) are not included in that pore volume model leading to lower porosities of the BJH approach than for absolute porosity measurements. [44]

Another approach is the direct deduction of the porosity as function of the BET specific surface area, which is a purely empirical relation, estimating u_j as system dependent tuning parameters. [45]

$$A_{\mathrm{BET}} = u_1 + u_2 \sin(u_3 \Phi) + \Phi \sin(u_4 \Phi^2) + \Phi \sin\left(u_5 \Phi \sin(u_6 \Phi^2)\right) - u_7 \sin(u_8 \Phi) \sin\left(\sin(u_9 \Phi^2)\right) \quad (2.5)$$

To understand some of the properties of NPCs formed from mesoporous nanoparticle scaffolds, the relationship between volume expansion and porosity should be noted. As visible in Figure 2.1a, the porosity for materials with a large pore volume shows less significant dependence of the porosity on the total volume.

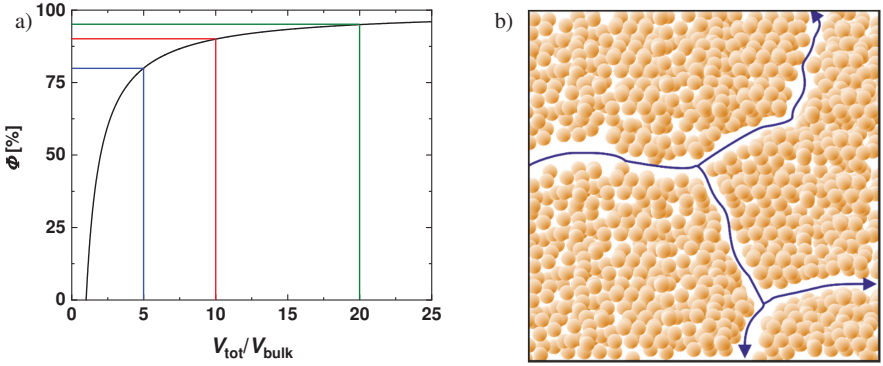

Figure 2.1. a) Evolvement of porosity Φ against volume ratio of structure. Normalized against non–porous bulk volume V_{bulk}. Color drop lines mark changes of porosity when doubling respective total volume. b) Two–dimensional intersection of a nanoparticle lattice including a bond percolation path (blue arrows) for channel diffusion through the network.

This is important in that way, that the structure might change in volume by a high factor but is only slightly changing porosity. Thus, the porosity is a rather insensitive parameter for samples with very high porosity. [40] Some material properties, e.g. electrical or thermal conductivity, or change transfer processes depend on the interconnectivity of the phases in the composite. [46] This cluster geometry is described by percolation theory, which defines under which conditions segregated clusters form a network by a statistical model. [47] The percolation threshold defines the critical probability at which global connectivity is reached, such as all phase areas of the same phase class are connected with each other. [48] This critical percolation threshold marks a geometrical phase transition.

[49] This is exemplarily shown for particle lattice with a percolating void network in Figure 2.1b. The nanoparticle clusters are divided by the void channel in two dimensions. However, in three–dimensional space, the clusters continue *via* bond percolation around the void channels. In a multiple phase system, reaching percolation is mandatory for establishing continuum processes, like conductivity. [50]

2.2 Silane Coupling Agents for Composites

The chemistry of functional silanes[3] is a versatile tool to tailor surface properties of macroscopic and microscopic bodies.[52–56] Silanes form oligomers through condensation reactions. [57] Even though it appears to be rather complex to control the reaction outcome during the synthesis of silane–based polymers, the applicability of their general properties is independent of the particular polymer structure, like good adhesion, level of hydrophobicity and thermal stability.[58–63] Therefore, silane chemistry is widely applied and accepted, although a detailed control of reaction is particulately difficult. [64]

The oligomers formed from silane monomers can be applied onto chalcogenide nanoparticles to either change their surface chemistry by adhesion of the silane moieties or to chemically link the nanoparticles with each other. [65] Since the silane hydrolysis reaction is an equilibrium reaction, functional groups are introduced which allow to quench reactivity of the silane moiety ending in a dense network of two independent polymeric linkages. [66] Due to their versatile chemical substituents, silanes are also applied for surface modification of inorganic semiconducting nanoparticles in sensor development. [67]

[2–(3,4–Epoxycyclohexyl)ethyl]trimethoxy silane (ECHTMO) and 3–(trimethoxy silyl)propyl methacrylate (MEMO) are typical organofunctional siloxanes which provide three methoxy groups for hydrolysis. Figure 2.2 shows a simplified oligomerization scheme of silane–based binders caused by methoxy group hydrolysis. [34, 68] First, activated by acidic or basic hydrolysis of organofunctional silicon alkoxide precursors results in the formation of organofunctional silanols. In the second step, organofunctional oligo– and polysiloxanes are formed upon poly–condensation. [34]

Silane coupling agents serve between organic and inorganic materials as surfactant. [69] This purpose is explained by the following coupling mechanisms: First under the presence of water, the alkoxy moieties of the silane are hydrolyzed forming silanol groups while the

[3] In this work, the class of materials silane does not refer to the IUPAC nomenclature of Si_nH_m compounds. [51] We define silane as organosilicon compound SiR_4, where each organic group R may differ.

alcohol molecule is split off during this condensation reaction. After this, the silanol molecules migrate to the inorganic interphase, where the hydroxyl groups form hydrogen bonds with the inorganic, e.g., mineral surface. In addition, direct mostly ionic bonds are formed upon condensation of the silanol groups coordinated at the mineral surface. [70]

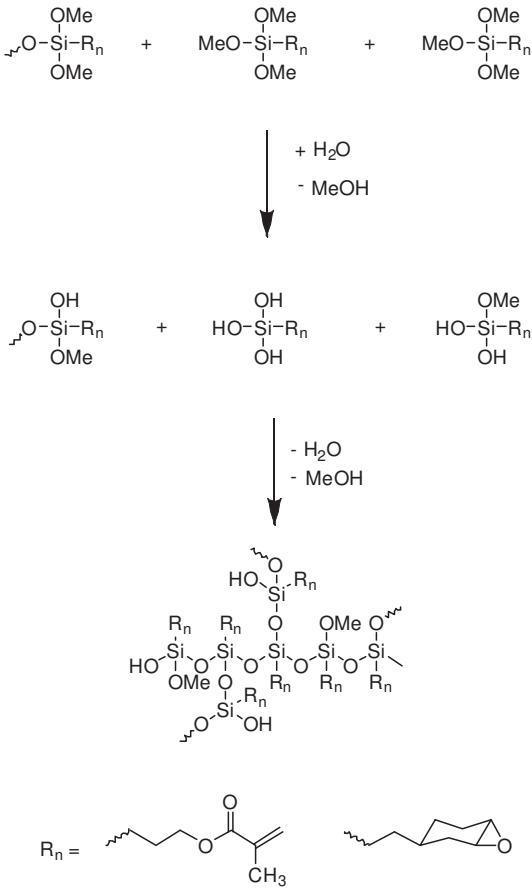

Figure 2.2. Simplified reaction scheme of sol–gel oligomerization of silanes under presence of water. Condensation product in each case is methanol. First, hydrolysis forms intermediate mixture from species with different degree of methoxylization of the silanes. Second, instable silanols condensate under water and methanol release to form the oligomeric binder. Studies were performed with MEMO (methacrylate–based) and ECHTMO (epoxy–based) binder.

The basic reaction scheme for the hydrolysis, condensation and oligomerization of silanes is presented in Figure 2.2. The organic segment of the silane, often used with an alkyl–